An analysis of Figure 4 also suggests that the $^3A'$ state of ketene may dissociate into triplet CH_2 ($^3B_1$) and a vibrationally excited CO molecule. It is also reasonable to expect that the $^3A''$ state dissociates to the same products, especially since it is known experimentally that the next excited triplet state of CH_2 is approximately 8.7 eV above the $^3B_1$ state,[13] and would not appear to be accessible from either of the low-energy triplet states of ketene. The dissociation of the $^1A''$ state to CH_2 ($^1B_1$) and vibrationally excited CO is also apparent from Figure 4. This does not preclude the possibility of other excited singlet states of ketene dissociating to the same products. It might even be expected that the singlet state corresponding to the vertical $^3A_1$ state would be of importance in the photochemistry of this molecule.[19]

It is known experimentally that irradiation of ketene between 2700 and 2900 Å (4.29–4.59 eV) produces almost exclusively singlet CH_2.[20] Undoubtedly excitation to the $^1A''$ state is important in this process. Moreover, the almost exclusive production of singlet CH_2 suggests that only a few molecules are excited to the $^3A_1(^3A')$ state at these wavelengths. At longer wavelengths, irradiation of ketene produces an increasing amount of triplet CH_2. At 3660 Å (3.39 eV) the ratio of triplet to singlet CH_2 is 0.4, while between 3460 and 3820 Å (3.25–3.58 eV) the ratio becomes greater than 0.5.[20] These data suggest that the $^3A''$ state does indeed dissociate to triplet CH_2. However, the fact that singlet CH_2 is also formed at longer wavelengths indicates that the dissociation energy for the $^1A''$ state may be lower than indicated in Figure 4.

(19) No calculations for the excited $^1A_1$ state have been reported here since it has already been demonstrated in ref 9 that a larger basis set than that used in this work is necessary to obtain even a moderate approximation to singlet $\pi \rightarrow \pi^*$ excitation energies.

(20) J. W. Calvert and J. N. Pitts, "Photochemistry," Wiley, New York, N. Y., 1967.

Conclusions

On the basis of the calculations performed in this study, it is possible to draw the following tentative conclusions. 1. The two low-energy bands of the ketene spectrum arise from $^3A''(^3A_2) \leftarrow {}^1A_1$ and $^1A''(^1A_2) \leftarrow {}^1A_1$ excitations, respectively. The transition giving rise to these states is not, however, analogous to the low-energy transition observed in formaldehyde. 2. In the $^3A''$ and $^1A''$ states, ketene has planar molecular C_s symmetry, in which the C–O bond is strongly bent in the molecular plane, and the C–C and C–O bonds are lengthened. 3. The lowest energy triplet state of ketene is of $^3A'$ symmetry in point group C_s (nonplanar) and is characterized by a very long C–C bond. For large C–C bond distances, this state is the lowest energy state in ketene. Because of the difference between the vertical excitation energy and the 0–0 energy for the $^3A'(^3A_1) \leftarrow {}^1A_1$ excitation, the relaxed $^3A'$ state may not be formed directly by absorption of energy from the ground state. 4. Dissociation may occur from the $^3A'$ and $^3A''$ states of ketene yielding CH_2 ($^3B_1$) and vibrationally excited CO. The $^1A''$ state may also dissociate, giving CH_2 ($^1B_1$) and CO.

Acknowledgments. Thanks are due to Dr. Ronald Jonas and the staff of the Youngstown State University Computer Center for their generous and helpful cooperation in this project, to Dr. Howard Mettee for many valuable discussions on photochemistry, and to Mr. Gus Mavrigian for assistance with the error analysis.

Molecular Orbital Theory of E2 Reactions and Nuclear Magnetic Resonance Spin–Spin Coupling in Ethane-Like Molecules[1]

John P. Lowe

Contribution from the Department of Chemistry, The Pennsylvania State University, University Park, Pennsylvania 16802.
Received October 19, 1971

Abstract: Molecular orbital calculations of syn and anti modes of E2 reactions are analyzed in terms of current reactivity theories. The roles of charge polarization and charge transfer are analyzed. The effects of charge transfer appear to be only partly understandable in terms of the lowest empty MO of the substrate. The tendency for syn eliminations to proceed through a more E1cb-like transition state is shown to result in part from charge polarization produced by negative base. The torsional angle dependence of vicinal nmr spin–spin coupling in ethane is calculated and rationalized in terms of delocalized MO's. This phenomenon is shown to be closely related to the nature of charge delocalization into substituted ethanes by attacking base. As a result, there is good reason to expect strong nmr spin coupling between sites which are strongly coupled in E2 reactions.

When staggered haloethane undergoes base-assisted bimolecular elimination (E2 reaction), the base attacks and removes the proton trans planar from halogen X (anti elimination),[2,3] charge is transferred to the departing halide, the two carbons become sp^2 hybridized, and a π bond is formed. These processes proceed more or less concurrently, and the fact that, under anti attack, the incipient π lobes on the α and β

(1) Acknowledgment is made to the donors of the Petroleum Research Fund, administered by the American Chemical Society, for support of this research.

(2) J. F. Bunnett, *Surv. Progr. Chem.*, 5, 53 (1969).

(3) C. K. Ingold, "Structure and Mechanism in Organic Chemistry," 2nd ed, Cornell University Press, Ithaca, N. Y., 1969, Chapter 9.

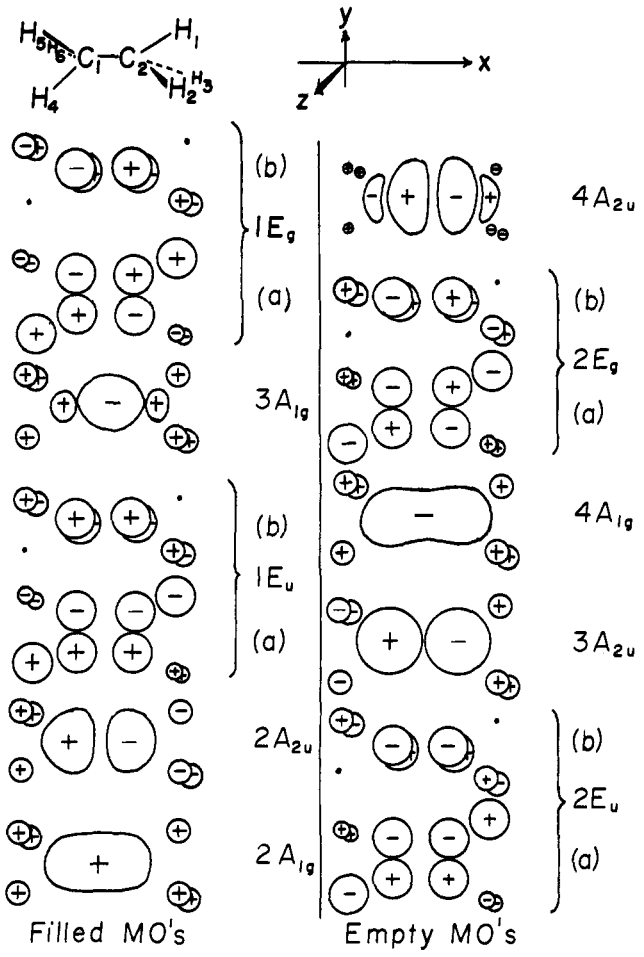

Figure 1. MO's of staggered ethane. Energy increases upward in each column.

carbons are coplanar, allowing π stabilization in the transition state, is generally taken as the reason for preferred removal of the trans rather than a gauche proton.

When eclipsed haloethane undergoes E2 reaction, the cis-coplanar hydrogen is eliminated[4] for the same reason (syn elimination). The fact that anti elimination is more common than syn elimination is only partly ascribable to the greater frequency of staggered conformations over eclipsed ones. It now seems well established[5,6] that syn eliminations proceed along the reaction coordinate in a less synchronous manner than do anti eliminations. The extent of C–H bond stretching is relatively greater in the syn mode transition state; the extent of C–X bond stretching is relatively less. The loss of synchronization delays the onset of π stabilization and is, presumably, another factor responsible for the greater ease of anti elimination.

In this paper we describe molecular orbital (MO) calculations which (1) give insight into the reason for the different natures of syn and anti mode transition states, (2) clarify a relation between E2 stereochemistry and vicinal nmr spin–spin coupling, and (3) show the desirability for explicit consideration of polarization effects in the MO treatment of certain reactions.

(4) This statement is based on indirect evidence from studies on other reactions.

(5) D. S. Bailey and W. H. Saunders, Jr., *J. Amer. Chem. Soc.*, **92**, 6904 (1970).

(6) G. Biale, A. J. Parker, S. G. Smith, I. D. R. Stevens, and S. Winstein, *ibid.*, **92**, 115 (1970).

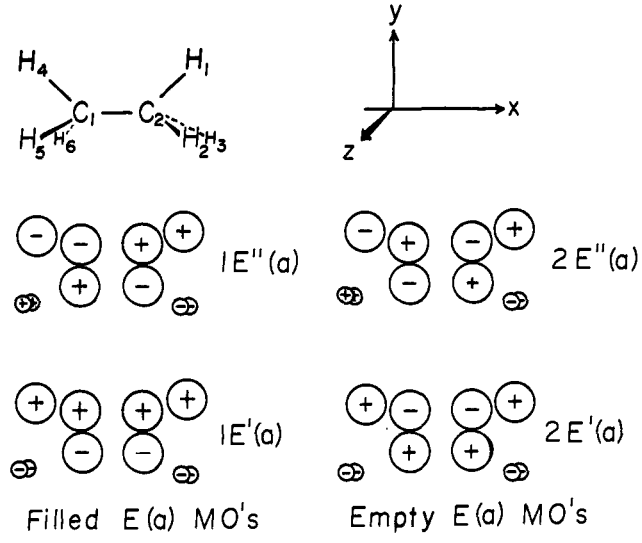

Figure 2. Some MO's of eclipsed ethane.

Molecular Orbitals of Ethane. The high symmetries of staggered (D_{3d}) and eclipsed (D_{3h}) ethane determine most of the qualitative features of the minimal valence basis set MO's. (See Figures 1 and 2, Tables I and II. Data for eclipsed ethane will be presented in an abbreviated form throughout this paper.) Since both forms possess a C_3 axis, the MO's of A symmetry (nondegenerate MO's) must have identical coefficients for all hydrogen 1s atomic orbitals (AO's) on a given methyl group. The MO's of E symmetry (doubly degenerate) are transformable to the forms shown and tabulated here, wherein (a) the 1s AO's on two methyl protons have identical coefficients (c_a) while that on the third has coefficient $-2c_a$, or (b) two methyl protons have 1s AO coefficients of equal magnitude but opposite sign ($+c_b, -c_b$) while the third has a coefficient of zero. These three symmetry-allowed methyl-hydrogen orbitals combine with carbon–carbon σ and π bonding and antibonding combinations as shown in Figures 1 and 2.

The first point to note is that the seven lowest energy MO's (the filled set) in either conformation are C–H bonding; the higher energy set (the empty set) are C–H antibonding. This is a feature which occurs in extended Hückel MO[7] (EHMO) calculations, CNDO/2 and INDO calculations,[8] and *ab initio* SCF–LCAO–MO calculations.[9] It is due to the fact that there are six C–H bonds and only one C–C bond. Within each set the ordering is partly predictable from simple considerations. For instance, the E_u and E′ levels, which are C–C π bonding, lie lower in energy than their π antibonding E_g or E″ mates. However, some switching of orbital levels does occur as we proceed from EHMO to CNDO/2 to INDO to *ab initio* methods of calculation. By these methods, the lowest empty MO (LEMO) in staggered ethane is, respectively, A_{2u}, E_u, A_{2u}, A_{1g}. Further changes could be introduced, within some of these methods, by varying the choice of parameters.

(7) R. Hoffmann, *J. Chem. Phys.*, **39**, 1397 (1963).

(8) J. A. Pople and D. L. Beveridge, "Approximate Molecular Orbital Theory," McGraw-Hill, New York, N. Y., 1970.

(9) R. M. Pitzer and W. N. Lipscomb, *J. Chem. Phys.*, **39**, 1995 (1963).

Table I. CNDO/2 MO's for Staggered Ethane[a]

AO	MO no. and symmetry: 1 $2A_{1g}$	2 $2A_{2u}$	3 $1E_u(a)$	4 $1E_u(b)$	5 $3A_{1g}$	6 $1E_g(a)$	7 $1E_g(b)$	8 $2E_u(a)$	9 $2E_u(b)$	10 $3A_{2u}$	11 $4A_{1g}$	12 $2E_g(a)$	13 $2E_g(b)$	14 $4A_{2u}$
1 C_s	−0.563	0.437	0	0	0.029	0	0	0	0	0.498	−0.426	0	0	0.247
C_x	−0.154	−0.283	0	0	0.644	0	0	0	0	−0.072	0.247	0	0	0.644
C_y	0	0	−0.536	0	0	−0.448	0	−0.462	0	0	0	−0.547	0	0
C_z	0	0	0	0.536	0	0	−0.448	0	−0.462	0	0	0	−0.547	0
2 C_s	−0.563	−0.437	0	0	0.029	0	0	0	0	−0.498	−0.426	0	0	−0.247
C_x	0.154	−0.283	0	0	−0.644	0	0	0	0	−0.072	−0.247	0	0	0.644
C_y	0	0	−0.536	0	0	0.488	0	−0.462	0	0	0	0.547	0	0
C_z	0	0	0	0.536	0	0	0.448	0	−0.462	0	0	0	0.547	0
H_1	−0.230	−0.276	−0.377	0	−0.167	0.447	0	0.437	0	0.287	0.293	−0.366	0	−0.089
H_2	−0.230	−0.276	0.188	0.326	−0.167	−0.223	0.387	−0.219	0.379	0.287	0.293	0.183	−0.317	−0.089
H_3	−0.230	−0.276	0.188	−0.326	−0.167	−0.223	−0.387	−0.219	−0.379	0.287	0.293	0.183	0.317	−0.089
H_4	−0.230	0.276	0.377	0	−0.167	0.447	0	−0.437	0	−0.287	0.293	−0.366	0	0.089
H_5	−0.230	0.276	−0.188	0.326	−0.167	−0.223	−0.387	0.219	0.379	−0.287	0.293	0.183	0.317	0.089
H_6	−0.230	0.276	−0.188	−0.326	−0.167	−0.223	0.387	0.219	−0.379	−0.287	0.293	0.183	−0.317	0.089
MO energy (au)	−1.4767	−1.0683	−0.8622		−0.6684	−0.5998		0.2859		0.2916	0.3106	0.3701		0.3930

[a] See Figure 1 for atom numbering scheme and coordinate orientation.

Table II. CNDO/2 MO's for Eclipsed Ethane[a,b]

AO	MO no. and symmetry: 1 $2A_1'$	2 $2A_2''$	3 $1E'(a)$	4 $1E'(b)$	5 $3A_1'$	6 $1E''(a)$	7 $1E''(b)$	8 $2E'(a)$	9 $2E'(b)$	10 $3A_2''$	11 $4A_1'$	12 $2E''(a)$	13 $2E''(b)$	14 $4A_2''$
1 C_s	0.563	−0.437	0	0	−0.029	0	0	0	0	−0.498	−0.427	0	0	−0.246
C_x	0.154	0.283	0	0	−0.644	0	0	0	0	0.071	0.248	0	0	−0.644
C_y	0	0	0.535	0	0	−0.449	0	−0.463	0	0	0	0.546	0	0
C_z	0	0	0	−0.535	0	0	−0.449	0	0.463	0	0	0	0.546	0
H_4	0.2303	−0.276	0.378	0	0.168	−0.446	0	0.436	0	0.287	0.292	−0.367	0	−0.090
H_5	0.2303	−0.276	−0.189	−0.327	0.168	0.223	−0.386	−0.218	−0.378	0.287	0.292	0.183	−0.318	−0.090
H_6	0.2303	−0.276	−0.189	0.327	0.168	0.223	0.386	−0.218	0.378	0.287	0.292	0.183	0.318	−0.090
MO energy (au)	−1.4769	−1.0676	−0.8635		−0.6684	−0.5978		0.2842		0.2924	0.3101	0.3715		0.3932

[a] Coefficients for C_2 and $H_{1,2,3}$ can be generated by symmetry. [b] See Figure 2 for atom numbering scheme and coordinate orientation.

Table III. Changes in Unnormalized[a] Overlap Populations in Ethane, Induced by Hydride Ion Approach

	Staggered			Eclipsed		
	R = 4 Å	1.5 Å	HOMO (1.5 Å)	4 Å	1.5 Å	HOMO (1.5 Å)
C_1–C_2						
s–s	−0.0001	−0.0016	−0.0014	−0.0001	−0.0014	−0.0011
s–p_x	−0.0001	−0.0017	−0.0021	0.0000	−0.0018	−0.0024
p_x–p_x	−0.0001	−0.0005	+0.0016	−0.0001	−0.0005	+0.0017
p_y–p_y	−0.0001	+0.0038	+0.0019	−0.0004	+0.0036	+0.0028
p_z–p_z	+0.0002	+0.0012	0.0	+0.0004	+0.0016	0.0
Total	−0.0002	+0.0012	0.0000	−0.0002	+0.0015	+0.0010
C_2–H_1						
s–s	+0.0047	−0.0028	−0.0074	+0.0046	−0.0029	−0.0077
p_x–s	−0.0004	−0.0067	−0.0014	−0.0004	−0.0068	−0.0014
p_y–s	−0.0026	−0.0494	−0.0103	−0.0025	−0.0494	−0.0107
Total	+0.0017	−0.0589	−0.0191	+0.0017	−0.0591	−0.0198
C_1–H_4						
s–s	−0.0026	−0.0075	−0.0009	+0.0018	+0.0031	+0.0007
p_x–s	+0.0004	+0.0026	+0.0006	+0.0003	+0.0008	−0.0006
p_y–s	+0.0006	−0.0025	−0.0013	−0.0012	−0.0049	−0.0017
Total	−0.0016	−0.0074	−0.0016	+0.0009	−0.0010	−0.0016

[a] Calculated using CNDO/2 coefficients, for which $C^+C = 1 \mp C^+SC$. See footnote 12.

Molecular Orbital Calculations on E2 Reactions. The MO theory for chemical reactions such as these focuses on the nature of the substrate MO into which electrons flow from the attacking base.[10,11] The extent of participation by a given empty MO of the substrate is usually argued, on the basis of perturbation theory, to roughly depend on the overlap between that MO and a filled MO of the base, and also on the difference in orbital energy levels between these MO's. This energy factor normally is expected to strongly favor participation by one or more of the LEMO's of the substrate.

Examination of Figures 1 and 2 shows that there is indeed one low-lying empty MO ($2E_u$(a) or 2E′(a)) which is C–C π bonding and strongly C–H antibonding in a coplanar pair of C–H bonds. Partial occupation of this MO would tend to carry the system along the E2 reaction coordinate. While the existence of this low-lying empty MO provides a tempting explanation for the preference for anti or syn elimination over gauche elimination, it does not give any hint that the transition state for the two modes should differ in any substantial way.

We have performed a number of CNDO/2 calculations for various simulated E2 reactions. We chose the CNDO/2 method because the EHMO method neglects charge repulsion, which we felt might be important for calculations involving a charged base. In Table III are given changes in unnormalized bond populations[12] produced when a hydride ion approaches staggered or eclipsed ethane along the C_2–H_1 bond axis. (See Figures 1 and 2 for numbering scheme.) When the hydride ion is 4 Å beyond H_1 (R = 4 Å), no significant charge transfer from hydride to ethane occurs (in a CNDO/2 calculation), so the changes in bond population at this point are due to charge polarization in ethane by the negative base. When the hydride is much closer (R = 1.5 Å) significant charge transfer occurs, so changes in bond populations are now attributable to both polarization and charge transfer. Most (but not all) of the charge transfer involves the highest occupied MO (HOMO) of the hydride–ethane complex. The contributions to bond populations due to this HOMO alone are also tabulated in Table III. Inspection of Table III leads to the following conclusions. (1) Most of the individual contributions to bond population changes at R = 1.5 Å are quite different from those due to the HOMO alone. (2) Most of the net effects at R = 1.5 Å appear reasonably consistent with the effects expected to result from the HOMO plus polarization, polarization being assumed greater at 1.5 than at 4 Å. (The change in p_z populations is entirely due to polarization, for reasons of symmetry.) (3) The net population change *in each bond*, as given by the HOMO, is fairly similar for syn and anti attack, whereas the changes due to all MO's show a much greater weakening of the leaving group in the anti mode. Evidently, the most significant effect due to polarization is its tendency to weaken the anti C–H (leaving) bond but to strengthen the syn (leaving) bond. The additional equal weakening of both bonds by the HOMO, due to charge transfer, results in the syn bond being weakened but still not so much as the anti bond.

The strengthening of the syn bond by polarization is similar to the effect described earlier, in our analysis of SN2 reactions, where we found that C–H bonds which are polarized *positive* are strengthened, whereas bonds wherein the H is polarized negative are weakened. At R = 4 Å, before any charge transfer occurs, the hydrogen cis coplanar to the attacked hydrogen in eclipsed ethane *is* calculated to be more positive than in unperturbed ethane. At R = 1.5 Å, it is more negative than in the unperturbed case, but it is much less negative than is its anti mode analog. Thus, charge transfer has more than copensated for the loss due to polarization, but polarization is still present and has an important effect on relative bond populations and relative charges.

(10) K. Fukui, H. Hao, and H. Fujimoto, *Bull. Chem. Soc. Jap.*, 24, 348 (1969), and references cited therein; G. Klopman and R. F. Hudson, *Theor. Chim. Acta*, 8, 165 (1967); G. Klopman, *J. Amer. Chem. Soc.*, 90, 223 (1968); R. G. Pearson, *ibid.*, 91, 1252 (1969).

(11) L. Salem, *ibid.*, 90, 543, 553 (1968); *Chem. Brit.*, 5, 449 (1969).

(12) R. S. Mulliken, *J. Chem. Phys.*, 23, 1833, 1841 (1955). The coefficients used in calculating these populations are normalized so that $C^+C = 1$ whereas the Mulliken formulation is consistent with $C^+SC = 1$. Our experience (ref 13) has been that renormalization changes population magnitudes but not the qualitative relationships among them. Hence these values are somewhat similar to the bond orders of simple Hückel theory since, there also, the sum of bond orders and charge densities does not add up to the total number of electrons.

Table IV. Changes in Mulliken Overlap Populations in Fluoroethane, Induced by Fluoride Approach

	Staggered			Eclipsed		
	R = 4 Å	1.5 Å	HOMO (1.5 Å)	R = 4 Å	1.5 Å	HOMO (1.5 Å)
C–C	+0.0007	+0.0070	+0.0021	+0.0008	+0.0064	+0.0012
C_2–H_1	+0.0007	−0.1247	−0.0346	+0.0002	−0.1324	−0.0414
C_1–F	−0.0034	−0.0140	−0.0043	+0.0018	−0.0045	−0.0026

Table V. Effects on E2 Reactions Expected from Charge-Transfer-Induced Changes in Electrostatic Interactions

Initial charge		Polarization effects		Charge effects	
B	X	Mode favored	Mode made more Elcb	Mode favored	Mode made more Elcb
−1	0	Anti	Syn	Anti	Syn
−1	+1	Anti	Syn	Anti	Syn
0	0	Neither	Neither	Syn	Anti
0	+1	Neither	Neither	Anti	Syn

These calculations cannot give an accurate measure of the relative importance of charge transfer and polarization because the calculations do not allow for the diffuseness of a negative ion such as H^-, so the orbital overlap leading to charge transfer is systematically underestimated.

We can resolve the newly occupied (R = 1.5 Å) HOMO over the ethane substrate into the unperturbed MO's of ethane.[13] This will show how much it resembles the LEMO of ethane. This resolution for staggered ethane is displayed in Figure 3. The eclipsed

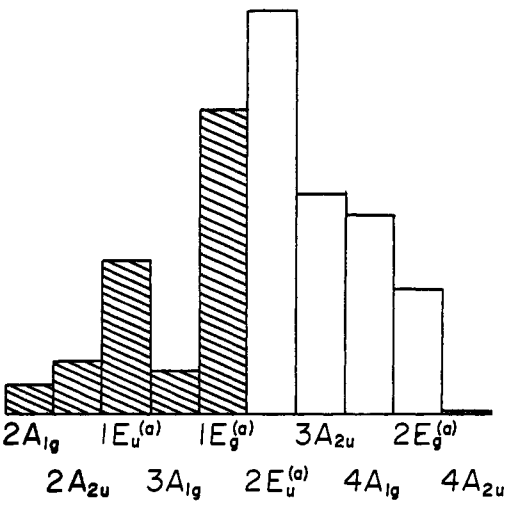

Figure 3. Relative amounts of MO's (φ_i) of unperturbed staggered ethane present in HOMO of hydride–ethane complex. The shaded bars correspond to MO's in the filled set. The E(b) contributions are zero by symmetry. The bar heights give relative magnitudes of c_i^2, where HOMO = $\Sigma_i c_i \varphi_i$. The profile for the HOMO for syn attack on eclipsed ethane is almost identical.

resolution is almost identical. The HOMO is seen to be a linear combination of filled and empty unperturbed MO's. While it is true that the $2E_u$(a) MO is the largest single component of the charge transfer MO, it is also true that other MO's are present in significant amounts. This is unfortunate from a theoretical point of view, because it prevents us from merely taking the bond properties of the $2E_u$(a) MO as being identical with the effects of charge transfer. This is disallowed, not only because $2E_u$(a) has companions which will contribute, but because, when the HOMO is squared, cross terms between the unperturbed MO's will contribute to bond populations.[13] The fact that the HOMO contributions to population changes in the C_2–H_1 and C_1–H_4 bonds differ by an order of magnitude is one manifestation of this situation.

The attack by F^- on fluoroethane has been analyzed in a similar way. An abbreviated tabulation of population changes is given in Table IV. Broadly speaking, the same conclusions pertain, except the nature of the HOMO at 1.5 Å shows more difference between the syn and anti modes. However, because the fluoride ion has several occupied AO's, not all at the same energy, it is questionable whether identifying the charge-transfer effect with a single MO is very meaningful.[14]

Note that the polarization effect should operate regardless of whether a negative base attacks a CH_3CH_2X molecule or a $CH_3CH_2NR_3^+$ molecule. In either case, the negative base tends to repel electrons to the most distant parts of the molecule. For syn elimination this retards electron transfer to the leaving group, while for anti elimination it accelerates it.

The preceding discussion pertains to the early stages of a reaction wherein a negative base attacks a neutral or positive substrate. What if the base is neutral? Does the resulting absence of polarization mean that nonsynchronous behavior of syn eliminations should disappear? To answer this question, we must consider the reaction at a later stage, when significant transfer of charge to the leaving group has occurred. If B is the attacking base and X is the molecular group which is destined to leave then, as the reaction proceeds, B gains a proton and becomes more positive by one unit of charge, and X gains an electron. B can initially be negative or neutral, X can be neutral or positive. This leads to four cases altogether. For example, if initially X is positive and B is negative, the reaction proceeds toward zero charge for each, and an attractive interaction is lost. This should contribute positively to the activation energy, and more so in the syn mode, thus favoring anti elimination. If a syn elimination does occur, the nonsynchronous mechanism should

(13) J. P. Lowe, *J. Amer. Chem. Soc.*, **94**, 60 (1972).

(14) In each occupied MO, the percentage of charge placed in AO's of the attacking fluoride is, starting with the HOMO, 87, 100, 100, 0, 0, 8, 0, 26, 58, 3, 0.

reduce the rate of loss of attractive interaction, so the charge situation favors anti over syn and favors syn being nonsynchronous relative to anti. Similar analysis of the other three cases leads to the results summarized in Table V. The effects due to polarization, when present, are qualitatively the same as the effects expected from charges. For neutral base, we see that there is reason to expect less tendency for the syn mode to be as nonsynchronous. In fact, for B and X neutral, the charge effect would seem to favor a syn elimination.[15]

Many factors enter the determination of activation energies and frequency factors. We have no basis for claiming that this charge effect will dominate mode selection. However, it may be possible to find systematic differences between E2 reactions involving charged *vs.* uncharged bases, differences ascribable to the charge effect. We have made a preliminary test of this notion by calculating the CNDO/2 wave functions for syn and anti attack by ammonia on fluoroethane (R = 1.5 Å). The extent of C–F bond weakening as measured by population is slightly greater for the syn mode, consistent with Table V. However, weakening of the attacked C–H bond remains greater for syn attack. Thus, while the syn mode might still be less synchronous than the anti mode, it seems possible that the anti mode under neutral base attack is less synchronous than is the anti mode under negative base attack. We emphasize that these last two paragraphs are speculative.

Vicinal Spin–Spin Coupling in Ethane and Fluoroethane. It has been pointed out[16] that nmr spin–spin coupling constants can be correlated with reaction rates or stereochemistries in many instances. In order to examine such a connection for E2 reactions, we first examine the vicinal spin–spin coupling in ethane and fluoroethane.

The Karplus curve,[17,18] relating vicinal proton–proton coupling in ethane with torsional angle, shows strongest coupling at angles 180 and 0°. This angle dependence is predicted by valence bond[17] and MO[18] calculations and is consistent with experimental results.[19] It now appears[20] that a similar curve describes vicinal H–F coupling, suggesting that, for light elements, the angular dependence of vicinal coupling is not strongly dependent on the nature of the substituent (except for the nuclear spin requirement).

The physical process which couples the nuclear spins of two protons may be pictured as follows. Suppose a proton (H_1) is in a spin orientation which causes it to be slightly more attractive for an electron having spin α. Then some slight electron spin polarization will occur so that there is a higher amount of α spin than β spin at H_1. This leads to a relative deficiency of α spin elsewhere (for a singlet molecule) so some other proton (H_4) may find itself surrounded by an excess of β spin and hence "prefer" a nuclear spin orientation attractive to β spin. Thus the energy of a given nuclear spin orientation for H_4 is influenced by the orientation at H_1; they are coupled. If the polarization of electron spin to H_1 removes more spin density from H_4 than from H_5, H_1 and H_4 are more strongly coupled than H_1 and H_5. Thus, MO theory of nmr spin–spin coupling depends on an intrinsic molecular spin polarizability.

Polarization is effected by mixing some of the empty MO's into the filled set. For example, referring to the MO's of staggered ethane, if a perturbation tends to reduce the size of an MO at H_1, we might expect MO $1E_g(a)$ to combine with the negative of $2E_u(a)$. In addition to producing the requisite reduction at H_1, this will produce an enhanced coefficient for hydrogens on the other methyl group but principally on the trans coplanar hydrogen, H_4. (The $1E''(a)$–$2E'(a)$ combination plays the analogous role in eclipsed ethane.) This is an example of but one of the many interactions involved in the approximate MO perturbational expression for the spin–spin coupling constant, $\mathcal{J}_{kl}$.

$$\mathcal{J}_{kl} = \text{constant} \times \sum_{i=1}^{\text{occ}} \sum_{j=\text{LEMO}}^{\text{unocc}} \left(\frac{c_{il}c_{jl}}{\epsilon_j - \epsilon_i - J_{ij}} \right) c_{ik}c_{jk} \quad (1)$$

This expression is simply a constant times the spin polarizability.[18] The indices l and k refer to the 1s AO's on the coupled protons. The ϵ's are the orbital energies, and J_{ij} is the repulsion between an electron in the filled-set MO i and an electron in the empty-set MO j. (In Hückel-type theories, J_{ij} would not appear.) The term in parentheses indicates the extent to which MO's i and j interact to move charge to or from AO l. The rest of the sum indicates the extent to which the activity at AO l will be transmitted to AO k. (Only the Fermi contact interaction is being considered here. We neglect contributions due to overlap of an AO based on one center with other nuclei.)

The squares of the various terms in *parentheses*, as calculated using CNDO/2 wave functions and energies for staggered ethane, appear in Table VI. Here, l is the AO on H_1 of Figure 1. By far the largest value occurs for the $1E_g(a)$–$2E_u(a)$ interaction cited above. However, other sizable interactions exist as well. If we sum the terms in Table VI by row and also by column, we arrive at an indication of the extent to which the various filled and empty MO's participate in shifting charge toward or away from H_1. These data are plotted in Figure 4. The relative participations of Figure 4 can be understood on the basis of coefficients and orbital energy differences. (Orbital energies for staggered ethane appear in Figure 5.) The $1E_g$–$2E_u(a)$ interaction is favored because these MO's lie close to the energy gap, so $\epsilon_j - \epsilon_i - J_{ij}$ is smallest for this interaction.[21] Notice that, in addition to the energy factor, the *coefficients* are of a nature to favor

(15) Effects of charge dispersion, creation, and annihilation have been correlated with the effect of solvent on rates of E2 reactions and with the ratio of SN2/E2 reaction. However, to our knowledge, the effects of this factor on the syn/anti ratio or on the degree of synchronization have not been considered.

(16) W. T. Dixon, *Tetrahedron Lett.*, 27, 2531 (1967); *Chem. Commun.*, 402 (1967); *Tetrahedron*, 24, 5509 (1968); C. H. DePuy, R. D. Thurn, and G. F. Morris, *J. Amer. Chem. Soc.*, 84, 1314 (1962).

(17) M. Karplus, *J. Chem. Phys.*, 30, 11 (1959); *J. Amer. Chem. Soc.*, 85, 2870 (1963).

(18) J. A. Pople and D. P. Santry, *Mol. Phys.*, 9, 301, 311 (1965). More rigorous treatment gives J as a perturbative sum involving triplet states. In MO theory, expression 1 works well in predicting the angular dependence of vicinal coupling provided proper descriptions are used for degenerate MO's. As we will show, this is because the vicinal coupling is greatly dependent on molecular symmetry, which is the one property that is correctly handled by all methods.

(19) A. A. Bothner-By, *Advan. Magn. Resonance*, 1, 195 (1965); M. Barfield and D. M. Grant, *ibid.*, 1, 149 (1965).

(20) K. L. Williamson, Y. F. Li Hsu, F. H. Hall, S. Swager, and M. S. Coulter, *J. Amer. Chem. Soc.*, 90, 6717 (1968).

(21) J_{ij} is fairly constant in these CNDO/2 calculations. An almost identical profile results when J_{ij} is omitted, although the vertical scale changes.

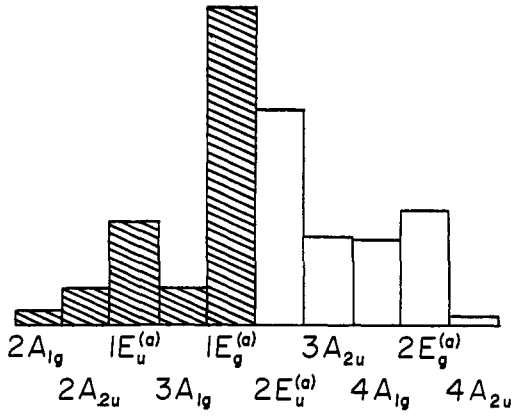

Figure 4. The data plotted are the row sums (shaded bars) and column sums of Table VI. E(b) MO's are excluded by symmetry.

$1E_g$–$2E_u$ over $1E_u$–$2E_g$. (Compare coefficients for H_1 in MO's 3, 6, 8, and 12 of Table I.) The reason for this will be discussed in the last section of this paper. Participation dies off for deeper lying filled MO's more than for higher lying empty MO's. This is mainly due

Table VI. Relative Importance of Various MO Interactions Produced by Nuclear Spin at H_1 in Staggered Ethane by CNDO/2 Method[a-c]

	Empty MO's					
Full MO's	$2E_u(a)$	$3A_{2u}$	$4A_{1g}$	$2E_g(a)$	$4A_{2u}$	Row sum
$2A_{1g}$	5.22	2.25	2.28	3.32	0.20	13.3 (13.3)
$2A_{2u}$	14.8	6.38	6.38	9.02	0.54	37.1 (37.2)
$1E_u(a)$	45.1	19.0	18.8	26.4	1.56	111 (111)
$3A_{1g}$	16.2	7.06	6.82	9.13	0.57	39.8 (39.9)
$1E_g(a)$	140.6	57.7	55.7	74.5	4.28	333 (337)
Column sum	222 (225)	92.4 (92.4)	90.0 (90.3)	122 (124)	7.15 (7.27)	

[a] Each entry is equal to 10^3 times the square of the term in parentheses in eq 1. [b] The figures in parentheses are the corresponding row and column sums obtained in the eclipsed ethane calculation. [c] Elements for rows and columns of E(b) type MO's are zero.

to the fact that the energy levels for the empty set are much more closely bunched than for the filled set in an SCF calculation. (See Figure 5.) The $3A_{2u}$ and $4A_{1g}$ MO'S are equally mixed in because their energies and 1s AO coefficients are very similar. MO's having coefficients of zero at H_1 do not participate at this level of perturbation theory.

Knowing that the $1E_g(a)$–$2E_u(a)$ (or $1E''(a)$–$2E'(a)$) interaction enters most strongly leads one (on the basis of our earlier argument) to expect strongest coupling between vicinal protons which are coplanar. That this is true can be seen from Table VII where the various values for the *entire* expression within the summation in expression 1 are tabulated for trans and 60° gauche vicinal protons in staggered ethane. Careful study of Table VII reveals that a rather simple understanding of the Karplus curve is possible. If we sum contributions by row and also by column, the total spin polarizability is given as the sum of the row sums, or, alternatively, as the sum of the column sums. But a simple situation

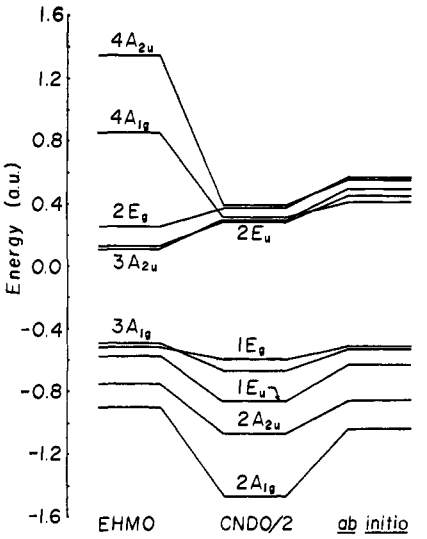

Figure 5. Energies of MO's of staggered ethane as produced by EHMO, CNDO/2, and *ab initio* methods.

exists among the column sums. The contributions due to $3A_{2u}$ and $4A_{1g}$ nearly cancel because they are mixed in about equally, as described above, and because g and u orbitals contribute oppositely to coupling. The $4A_{2u}$ MO contributes negligibly, due to its very small coefficients. This leaves the $2E_u(a)$ and $2E_g(a)$ MO's, and the former of these dominates. The $2E_u(a)$ MO interacts with all the filled MO's, but, once again, near cancellation among effects due to $2A_{1g}$, $2A_{2u}$, and $3A_{1g}$ leave only the $2E_u(a)$–$1E_g(a)$ and $2E_u(a)$–$1E_u(a)$ interactions. The former dominates. A similar analysis results if we start with the row sums and then analyze the dominant row ($1E_g(a)$) interactions with empty MO's. But now we can understand why gauche coupling is so much smaller than trans coupling. Comparing the data in Table IV for 180 *vs.* 60°, we see that the individual terms in the 60° set are equal to $^1/_4$, $^1/_2$, or 1 times the values in the 180° set, depending on whether the interaction is respectively E–E, E–A, or A–A. The approximate cancellation of effects due to MO's of A symmetry by row and by column largely removes the effect of A–A and E–A contributions, ultimately giving a gauche coupling of roughly $^1/_4$ the corresponding anti coupling. Thus, in the delocalized MO formulation of the problem, the major factor producing the Karplus curve is the two-to-one ratio of coefficients in E(a)-type MO's. The much greater size of the products for coefficients for coplanar hydrogens as opposed to gauche hydrogens is the delocalized MO equivalent to the partial π bonding cited by Pople and Santry[18] as the explanation in terms of localized orbitals. A similar analysis results from the data for 0 and 120° coupling in eclipsed ethane (not shown, but see footnote *b* of Table VII).

Calculations similar to those described above have been carried out for staggered and eclipsed fluoroethane. (The 2s AO on fluorine replaces a 1s AO on hydrogen in eq 1.) The spin polarizabilities thus calculated (and scaled up by 10^3) are: 0°, −1.166; 60°, −0.345; 120°, −0.397; 180°; −1.286. Since the constant in eq 1 is negative, these give positive values for $\mathcal{J}_{HF}$. Thus, the curve shape for vicinal H–F coupling is predicted by this method to be very much like

Table VII. Contributions of MO Interactions to 180 and 60° Vicinal Spin–Spin Polarizabilities in Staggered Ethane from CNDO/2 Wave Functions[a,b]

Full MO's	Empty MO's: $2E_u(a)$	$3A_{2u}$	$4A_{1g}$	$2E_g(a)$	$4A_{2u}$	Row sum
$2A_{1g}$	−7.27	−3.14	3.21	4.85	−0.290	−2.63
	(3.63)	(−3.14)	(3.21)	(−2.42)	(−0.290)	(0.998)
$2A_{2u}$	14.7	6.34	−6.46	−9.60	0.573	5.55
	(−7.35)	(6.34)	(−6.46)	(4.80)	(0.573)	(−2.10)
$1E_u(a)$	35.0	14.9	−15.1	−22.4	1.33	13.8
	(8.75)	(−7.47)	(7.57)	(−5.6)	(−0.665)	(2.59)
$3A_{1g}$	−9.32	−4.04	4.05	5.85	−0.356	−3.81
	(4.66)	(−4.04)	(4.05)	(−2.93)	(−0.356)	(1.39)
$1E_g(a)$	−73.2	−30.8	30.8	44.6	−2.61	−31.2
	(−18.3)	(15.4)	(−15.4)	(11.15)	(1.30)	(−5.88)
Column sum	−40.1	−16.7	16.5	23.3	−1.35	−18.3 (180°)
	(−8.61)	(7.09)	(−7.06)	(5.00)	(0.57)	−3.0 (60°)

[a] Each entry is equal to 10^3 times the sum in eq 1. 60° stereopolarizability terms are given in parentheses. Since the constant in eq 1 is negative, the spin couplings are positive. [b] The net polarizabilities (times 10^3) are entered at the bottom right of the Table. The corresponding values for eclipsed ethane are −14.1 at 0° and −5.2 at 120°.

that for vicinal H–H coupling. We have examined the tabulated values for term-by-term contributions but find no simple numerical relationships such as were found for ethane. A possible explanation for these results is that substitution of F for H mixes together the various A and E type MO's on the rest of the ethane frame but in a way that keeps the energy relationships roughly the same. That is, the HOMO of fluoroethane over the C_2H_5 fragment will be made up *primarily* of a linear combination of C_2H_5 fragments of the *higher* occupied MO's of unperturbed ethane. This would have the effect (observed here) of keeping the net coupling ratios about the same while scrambling the individual contributions and obscuring any simple explanation.

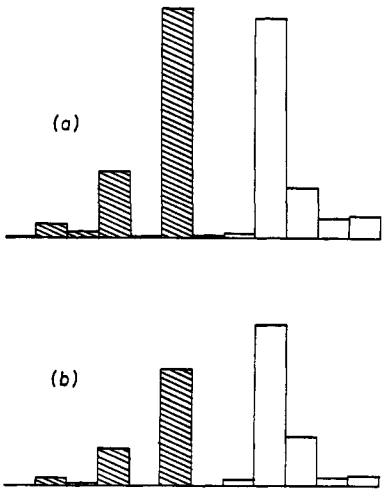

Figure 6. (a) Profile for spin-induced polarization in staggered fluoroethane. Perturbation occurs at H trans to F. (b) Profile for resolution of HOMO in anti attack by F^- on fluoroethane (R = 1.5 Å). MO's excluded by symmetry are not included in the profiles.

Connection between Reaction Coupling and Spin Coupling. We have seen that the perturbative mixing between filled and empty MO's induced by the nuclear spin at H_1 is determined by (1) the size of the MO at H_1, and (2) the denominator $\epsilon_j - \epsilon_i - J_{ij}$, which is *roughly* comparable to $\epsilon_j - \epsilon_i$ in behavior. We have seen that the MO into which base electrons are delocalized as the base approaches H_1 is made up of MO's from the filled and empty sets too. This mixture is roughly determined by (1) the overlap between each substrate MO with base MO's, and (2) the difference in energies between the base MO's and the substrate MO's.[10] Since the base normally should have an occupied MO energy somewhere near the energy gap between the filled and empty sets of the substrate, there is good reason for expecting these phenomena to bear some resemblance to each other.[16]

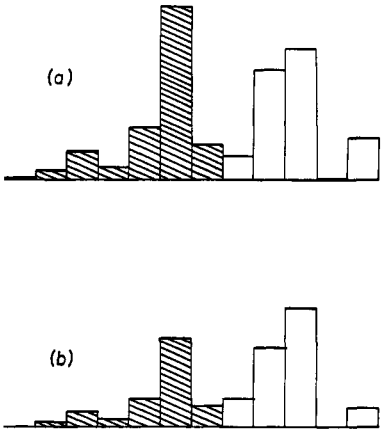

Figure 7. Same as Figure 6 except for eclipsed fluoroethane with (a) spin at H cis to F, (b) syn attack by F^- (R = 1.5 Å).

An example of such resemblance is provided by comparison of the spin-coupling profile for ethane (Figure 4) with the profile for the charge-transfer MO (Figure 3). Similar data for fluoroethane are plotted in Figures 6 and 7. In contrast to ethane, we find here a noticeable difference between the staggered and eclipsed profiles. But, for each conformation, the profiles for spin perturbation and base-attack perturbation are fairly similar. This leads to a *rough* rule: *A site which has strong positive spin coupling with a given proton is a site to which negative charge is preferentially transferred by the HOMO corresponding to base attack at that proton.*[16]

We have already indicated that polarization and charge–charge interactions can affect the reaction enough so that the HOMO is an incomplete indicator. For reactions in which a fair distance separates the at-

tacked and leaving groups, this should be less of a problem. The rule may thus be alternatively stated: *Given a site for a potential leaving group, and several fairly distant, topologically equivalent, but stereochemically distinct protons, the proton most likely to be extracted in an E2 reaction is the one with the largest positive coupling to the leaving group site, as measured with a proton or fluorine at that site.* This raises interesting possibilities for reactions involving charge transfer across the W-shaped bond linkage, which is well known[22] to be the orientation giving the strongest coupling through four bonds.

Some Comments on Theory. Great difficulty attends the direct computation of a reliable potential surface for reactions such as those considered here. CNDO/2 and EHMO energies are certainly too unreliable,[23] and even *ab initio* methods often fail when the wave function is restricted to a single configuration.[24] We have therefore avoided comparisons of energies. Even so, one must question the method independence of explanations based on an approximate method. In this section we discuss some of the relevant features of EHMO, CNDO/2, and *ab initio* SCF–LCAO–MO methods.

Arguments based on perturbation theory depend mainly upon MO energy level separation, MO symmetries, and coefficient sizes. Comparison of orbital energies for staggered ethane by the three methods of interest is made in Figure 5. The empty MO energies given by the EHMO approach are spread over a much greater energy range than are those given by the two SCF methods.[25] This suggests that the energy level differences between filled and empty MO's are very method dependent and that this parameter should be used cautiously in reactivity theories. In particular, Figure 5 makes it obvious that the unique importance of the LEMO would be difficult to defend on an energy basis in SCF cases. Examination of Figures 6b and 7b shows that more than one empty MO may be important, and the LEMO need not be one of these.

Among the filled MO's, CNDO/2 produces a greater energy spread than do the other methods.[26] Our spin calculation makes explicit use of the fact that $1E_u$ lies significantly below $1E_g$ in energy. Hence, we must consider how much our qualitative discussion of the angle dependence of vicinal spin–spin coupling depends on energy level differences and how much it depends on the AO coefficients.

In EHMO and *ab initio* methods, atomic overlap is included in the solution of the matrix equation $\mathbf{HC} = \mathbf{SCE}$, whereas it is neglected (*i.e.*, $\mathbf{S} = 1$) in the CNDO method. This has a noticeable effect on coefficient sizes, as Coulson has recently emphasized.[27] As more nodes appear in the orbitals, larger values for coefficients are needed to maintain normality when overlap is included. In Table VIII are tabulated the coefficients for the 1s AO on H_1 in the E(a)-type MO's as given by each method for staggered ethane. For the two methods which include overlap, coefficients for the *empty* MO's (both of which have nodes in each C–H bond) are markedly larger than coefficients of the filled MO's. In addition, for all three methods, the coefficients follow a pattern which forces the "energy neighbor" product of coefficients ($1E_g \times 2E_u$) to be larger than the other product, $1E_u \times 2E_g$. This coefficient pattern, most apparent for the CNDO/2 method, is just the σ molecular orbital equivalent to the corresponding Hückel π MO's of butadiene.[28] The lowest energy π MO of butadiene has smaller coefficients at the end atoms (0.371) than does the second lowest energy MO (0.600). This is because both MO's must vanish beyond the end atoms and the lower energy MO cannot change slope so rapidly. The two empty MO's must, by the pairing theorem,[29] show the reverse behavior. When overlap is included, this small-large–large-small pattern of coefficients is combined with the above-mentioned monotonic increase giving results like those in the first two columns of Table VIII. The combined effect of these two trends is to make the coefficients for the end-atom AO's considerably larger for the higher filled MO's than for the deeper ones, and also for (ground-state) empty MO's compared to filled MO's. This effect is independent of the number of atoms in the chain. It is likely to be a strong factor,[11] perhaps more important than orbital energies, in the success of methods, like the Woodward–Hoffmann approach,[30] which predict the nature of end-to-end interactions on the basis of the highest filled MO, both for ground and excited state molecules. Note, however, that the effect of overlap works *against* the coefficients on the terminal atoms of the LEMO dominating those from still higher empty MO's.

Table VIII. Coefficients for H_1 in E(a)-Type MO's in Staggered Ethane as Produced by Three Computational Methods

	EHMO	*Ab initio*	CNDO/2
$1E_u$	0.3448	0.3120	0.3770
$1E_g$	0.4089	0.4183	0.4466
$2E_u$	0.7225	0.7994	0.4372
$2E_g$	0.6991	0.7812	0.3658
$1E_g \times 2E_u$	0.2954	0.3344	0.1952
$1E_u \times 2E_g$	0.2410	0.2437	0.1379
$\frac{1E_g \times 2E_u}{1E_u \times 2E_g}$	1.22	1.37	1.41

The result of these considerations is that the coefficients favor perturbative dominance of the $1E_g$–$2E_u$ pair over the $1E_u$–$2E_g$ pair in all three calculations, but especially in CNDO/2 where overlap is neglected. This, coupled with the greater energy level spread in the filled set of CNDO/2 MO's, suggests that our qualitative explanation for the Karplus curve will at least partially

(22) M. Barfield, *J. Amer. Chem. Soc.*, **93**, 1066 (1971).
(23) E. I. Snyder, *ibid.*, **92**, 7529 (1970).
(24) A. C. Wahl and G. Das, *Advan. Quantum Chem.*, **5**, 261 (1970).
(25) The virtual MO's in SCF theory are orbitals which could be occupied by one additional electron moving in the potential field due to the (unperturbed) neutral molecule. We do not expect the energies for an electron in such orbitals to vary as much as energies for electrons in occupied MO's which are subject to more widely differing potentials. In the EHMO method, MO's attain their energies on the basis of number of nodes and placement of nodes, leading to energy level patterns similar to the pairing theorem behavior of simple Hückel theory. The continual addition of nodes, common to all three methods, leads to a blowing up of EHMO energies.
(26) This is probably due to underestimated interelectronic repulsion resulting from the approximations used in CNDO/2.
(27) C. A. Coulson, *Mol. Phys.*, **15**, 317 (1968).
(28) The methyl–hydrogen coefficients in E-type MO's of ethane are related to the terminal carbon AO's of butadiene through a hyperconjugation argument. See J. P. Lowe, *J. Amer. Chem. Soc.*, **92**, 3799 (1970), and references cited therein.
(29) L. Salem, "The Molecular Orbital Theory of Conjugated Systems," W. A. Benjamin, New York, N. Y., 1966.
(30) R. B. Woodward and R. Hoffmann, "The Conservation of Orbital Symmetry," Academic Press, New York, N. Y., 1970, p 44.

pertain for other methods but that the dominance of the $1E_g$–$2E_u$ interaction may be reduced. Also, it seems likely that cancellation of effects due to A-type MO's may be less complete due to changes in coefficients and orbital energies.[31]

(31) C. Barbier and G. Berthier, *Theor. Chim. Acta*, 14, 71 (1969); *Int. J. Quantum Chem.*, 1, 657 (1967).

Acknowledgments. It is a pleasure to thank Professors L. M. Jackman and J. E. Baldwin for drawing my attention to this problem. I also thank Professor R. M. Pitzer for making available the virtual MO's from his *ab initio* ethane calculation and Professors O. H. Crawford, J. A. Pople, W. H. Saunders, and J. F. Bunnett for helpful criticisms of the manuscript.

A Floating Spherical Gaussian Orbital Model of Molecular Structure. X. C_3 and C_4 Saturated Hydrocarbons and Cyclobutane

John L. Nelson and Arthur A. Frost*

Contribution from the Department of Chemistry, Northwestern University, Evanston, Illinois 60201. *Received November 15, 1971*

Abstract: The FSGO model is used to calculate geometries for three- and four-carbon hydrocarbons. By simply transferring, unchanged, most of the parameters from C_2H_6, the C–C–C bond angles for C_3H_8, *n*-C_4H_{10}, and *i*-C_4H_{10} are determined to be 112.5, 112.5, and 111.0°, respectively, in agreement with experiment within 0.3°. More complete minimization accurately predicts the detailed geometry of propane and cyclobutane. The differences in the C–H bond lengths and H–C–H bond angles in propane are predicted correctly. A D_{2d} structure is predicted for cyclobutane, with a dihedral angle of 32° and a tilt of 7° for the methylene groups.

The floating spherical Gaussian orbital (FSGO) model is discussed in detail in paper I of this series.[1] As currently applied, the model predicts the electronic and geometric structure of singlet ground states of molecules with localized orbitals without the use of any arbitrary or semiempirical parameters. The localized orbitals are constructed by using single normalized spherical Gaussian functions

$$\Phi(\vec{r} - \vec{R}_i) = (2/\pi\rho_i^2)^{3/4} \exp[-(\vec{r} - \vec{R}_i)^2/\rho_i^2]$$

with orbital radius, ρ_i, and position, R_i. A single Slater determinant represents the total electronic wave function. If S is the overlap matrix of the set of nonorthogonal localized orbitals Φ_i and $T = S^{-1}$, then the energy expression for a molecule is

$$E = 2\sum_{j,k}(j|k)T_{jk} + \sum_{k,l,p,q}(kl|pq)[2T_{kl}T_{pq} - T_{kq}T_{lp}]$$

where $(j|k) = \int\Phi_j h\Phi_k dv$ (h = one-electron operator) and $(kl|pq) = \int\Phi_k(1)\Phi_l(1)(1/r_{12})\Phi_p(2)\Phi_q(2)dv_1dv_2$. The energy is minimized by a direct search procedure with respect to all parameters: orbital radii, ρ_i, orbital positions, $\vec{R}_i$, and nuclear positions.

Previous work with the FSGO model[1] has indicated that the model works particularly well for molecules showing a high degree of covalency; in particular the hydrocarbons showed unusually good results.[2] With this in mind, work was extended to C_3 and C_4 saturated hydrocarbons and to cyclobutane. The emphasis in these studies is not toward calculation of accurate energies (simple FSGO typically gives about 85% of Hartree–Fock SCF values). Rather it is aimed at using the model as a tool for obtaining geometries (bond angles and bond length within 1–2%) and trends in rotation barriers (FSGO typically gives rotational barriers nearly twice experimental).

Investigation into these various hydrocarbons was taken at two distinct levels. First, an attempt was made to obtain rough geometries by simply transferring many of the parameters from smaller molecules (*e.g.*, propane from ethane). Typically the C–C bond lengths and the C–C–C bond angles are varied for each new molecule and rotational barriers are then calculated by assuming rigid rotation, not minimizing at the top of the barrier. (Stevens[3] has made a series of calculations on C_2H_6 and H_2O_2 and has concluded that rotational barriers can be calculated assuming rigid rotation if no lone pairs are present.) A second procedure involved determining details of the structure of propane and cyclobutane. These more extensive minimizations were carried out to test the simple FSGO's ability to conform with experimental results and to make predictions about geometries.

Transferability of Parameters

A method (hereafter termed SCF–FSGO) similar to the simple FSGO has been developed by Christoffersen and coworkers[4,5] for calculations on hydrocarbons. Here the concept of transferring parameters from smaller molecules and fragments has been used to construct large hydrocarbons. It would be instructive

(1) S. Y. Chu and A. A. Frost, *J. Chem. Phys.*, 54, 764 (1971); and references cited therein.

(2) A. A. Frost and R. A. Rouse, *J. Amer. Chem. Soc.*, 90, 1965 (1968).

(3) R. M. Stevens, *J. Chem. Phys.*, 52, 1397 (1970).

(4) (a) R. E. Christoffersen, *J. Amer. Chem. Soc.*, 93, 4104 (1971); (b) R. E. Christoffersen, D. W. Genson, and G. M. Maggiora, *J. Chem. Phys.*, 54, 239 (1971).

(5) G. M. Maggiora, D. W. Genson, R. E. Christoffersen, and B. V. Cheney, *Theor. Chim. Acta*, 22, 337 (1971).